Chinese Journal of Oceanology and Limnology
Vol. 33 No. 5, P. 1191-1200, 2015
http://dx.doi.org/10.1007/s00343-015-4136-4

Evaluation of wind vectors observed by HY-2A scatterometer using ocean buoy observations, ASCAT measurements, and numerical model data*

LI Dawei (李大伟)[1, 2], SHEN Hui (申辉)[1, **]

[1] *Institute of Oceanology, Chinese Academy of Sciences, Qingdao 266071, China*
[2] *University of Chinese Academy of Sciences, Beijing 100049, China*

Received Jun. 24, 2014; accepted in principle Oct. 2, 2014; accepted for publication Dec. 1, 2014

Abstract The first Chinese microwave ocean environment satellite HY-2A was launched successfully in August, 2011. This study presents a quality assessment of HY-2A scatterometer (HYSCAT) data based on comparison with ocean buoy data, the Advanced Scatterometer (ASCAT) data, and numerical model data from the National Centers for Environmental Prediction (NCEP). The in-situ observations include those from buoy arrays operated by the National Data Buoy Center (NDBC) and Tropical Atmosphere Ocean (TAO) project. Only buoys located offshore and in deep water were analyzed. The temporal and spatial collocation windows between HYSCAT data and buoy observations were 30 min and 25 km, respectively. The comparisons showed that the wind speeds and directions observed by HYSCAT agree well with the buoy data. The root-mean-squared errors (RMSEs) of wind speed and direction for the HYSCAT standard wind products are 1.90 m/s and 22.80°, respectively. For the HYSCAT-ASCAT comparison, the temporal and spatial differences were limited to 1 h and 25 km, respectively. This comparison yielded RMSEs of 1.68 m/s for wind speed and 19.1° for wind direction. We also compared HYSCAT winds with reanalysis data from NCEP. The results show that the RMSEs of wind speed and direction are 2.6 m/s and 26°, respectively. The global distribution of wind speed residuals (HYSCAT-NCEP) is also presented here for evaluation of the HYSCAT-retrieved wind field globally. Considering the large temporal and spatial differences of the collocated data, it is concluded that the HYSCAT-retrieved wind speed and direction met the mission requirements, which were 2 m/s and 20° for wind speeds in the range 2–24 m/s. These encouraging assessment results show that the wind data obtained from HYSCAT will be useful for the scientific community.

Keyword: HY-2A; scatterometer; wind fields; evaluation

1 INTRODUCTION

Near-surface wind vectors observed over the global oceans with high spatial resolution and frequent temporal sampling are of considerable interest, because wind speed and direction are fundamental parameters in various fields of meteorology, oceanography, and climate studies (Risien and Chelton, 2008). For example, they are utilized to study ocean surface waves, wind-driven current systems, and air-sea turbulent fluxes of momentum, heat, water vapor, and gases (Liu, 2002). Space-borne scatterometers can be utilized to extract high-resolution wind vectors in both space and time globally. The surface wind and stress fields derived from scatterometer observations can be applied to drive ocean circulation models at various scales and can be assimilated into regional and global numerical weather prediction models. However, it is necessary to validate the satellite wind data before they can be used for oceanic and meteorological studies.

Numerous studies have been conducted by comparing scatterometer-retrieved winds with in situ

* Supported by the National High Technology Research and Development Program of China (863 Program) (No. 2013AA09A505), the National Natural Science Foundation of China (No. 40906091), and the Open Project of School of Marine Sciences, Nanjing University of Information Science and Technology (No. KHYS1304)
** Corresponding author: shenhui@qdio.ac.cn

buoy and vessel observations to assess the quality of the wind data. In particular, previous studies have considered the Active Microwave Instrument on the European Remote Sensing Satellite (ERS/AMI) (Offiler, 1994), NASA scatterometer (NSCAT) (Bourassa et al., 1997; Ebuchi, 1999; Freilich and Dunbar, 1999; Masuko et al., 2000; Dickinson et al., 2001), and QuikSCAT (Draper and Long, 2002; Ebuchi et al., 2002; Bourassa et al., 2003; Chelton and Freilich, 2005).

The first Chinese microwave ocean environment satellite HY-2A was launched successfully in August, 2011. The scatterometer on board the HY-2A satellite (hereafter, HYSCAT) provides valuable measurements of sea surface wind fields. However, it is essential to validate the quality of the HYSCAT wind data before they can be assimilated into regional and global numerical weather prediction models, because biases in the retrieved wind field can alter model forcing and have an effect on the outputs of ocean circulation models. In the present study, wind vectors observed by HYSCAT are compared with other wind products to assess the quality of the HYSCAT-retrieved wind vectors. The paper is structured as follows. In Section 2, the data used in this paper are described. In Section 3, the results of comparison between the HYSCAT wind data and ocean buoy observations, the Advanced Scatterometer (ASCAT) measurements, and numerical model data are presented and discussed. The effects of oceanographic and atmospheric parameters on the scatterometer are also assessed using the buoy data. The conclusions are given in Section 4.

2 DATA

The data used in this study include in situ ocean buoy observations, satellite measurements, and numerical model data. The data are described in more detail in the following sections.

2.1 HYSCAT data

The HY-2A satellite is a sun-synchronous satellite orbiting at a height of 971 km with an inclination angle of 99.34°. Its local equator crossing time at the descending node is 6:00 AM. The orbital and recurrent periods of the orbit are 104.46 min and 14 days, respectively (Jiang et al., 2012). The mission carries a Ku-band scatterometer, a multi-band radiometer, and a dual-band altimeter. The scatterometer is a microwave instrument that measures global near-surface ocean wind speed and direction under all weather and cloud conditions. It uses a conical-scan rotating antenna with two pencil beams. The inner beam sweeps in a circular pattern with an incidence angle of 41° (HH-pol) and the outer beam sweeps at an incidence angle of 48° (VV-pol). The antennas radiate horizontally and vertically polarized microwave pulses at a frequency of 13.256 GHz and measure the electromagnetic radiation signal backscattered from the sea surface for several different azimuth angles (Dong et al., 2007). The measured sea surface Normalized Radar Cross Sections (NRCSs) were fitted to a geophysical model function (GMF) that relates the backscatter to neutral equivalent winds (Wentz and Smith, 1999; Hersbach et al., 2007; Li and Shen, 2014), to obtain the sea surface wind field at a height of 10 m above sea level. HYSCAT can measure wind vectors over a swath of 1700 km with a nominal spatial resolution of 25 km. Daily coverage is approximately 80% of the global oceans.

The HYSCAT data used in this paper are Operational Standard Data Products (Level 2B), which have been processed and distributed by the National Satellite Ocean Application Service (NSOAS). The reference height of the wind vectors is 10 m above the sea surface. Wind vectors have been retrieved with the empirical NSCAT-2 GMF. A Maximum Likelihood Estimator (MLE) (Long and Mendel, 1991) and the Median Filter Ambiguity Removal algorithm, which was initialized with the Numerical Weather Product (NWP), were used to select the most probable wind speed and direction. Only observations for which the rain flag algorithm did not detect rain were retained; these observations are considered in the following comparison exercise. The spatial resolution of the wind vector data is 25 km. Data observed during the period from January 1, 2012, to December 31, 2013, are included in this paper.

2.2 ASCAT data

The ASCAT scatterometer is a real aperture radar, operating at 5.255 GHz (C-band) and using vertically polarized antennas (http://www.eumetsat.int/website/home/Satellites/CurrentSatellites/Metop/MetopDesign/ASCAT/index.html). Its engineering design is notably different from that of HYSCAT. Rather than a rotating antenna, ASCAT has three fixed-beam antennas looking at 45° (fore-beam), 90° (mid-beam), and 135° (aft-beam) along the satellite track. The incidence angle varies from 34° to 64° for the outermost beams and 25° to 53° for the mid-beam. The antennas sweep out two 550 km swaths on both sides of the ground

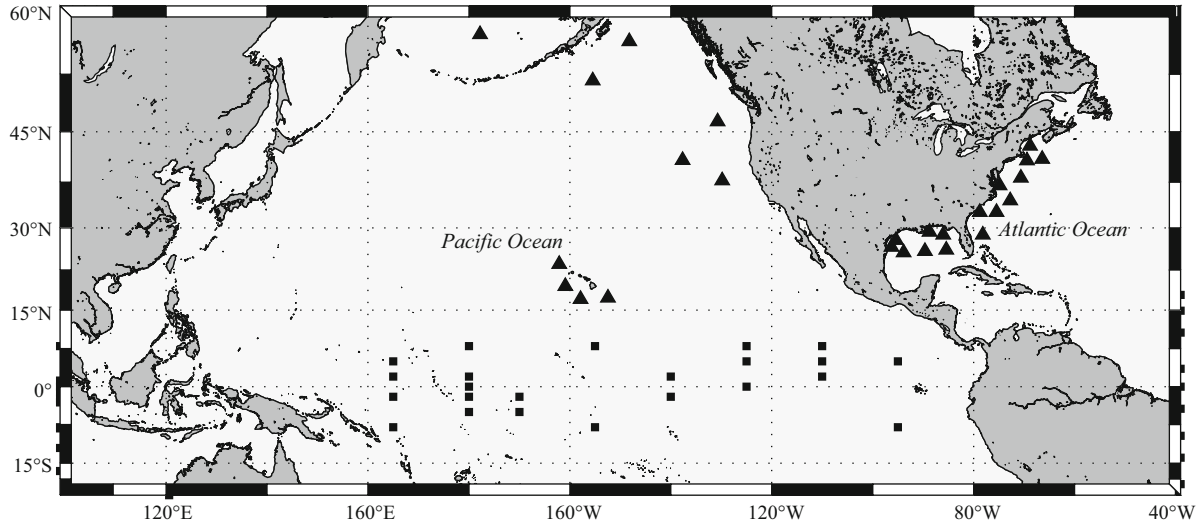

Fig.1 Location of the NDBC (triangles) and TAO (squares) buoys used in this study

track. Here, we use Level 2b ASCAT near-real-time data distributed by EUMETSAT and KNMI at a resolution of 25×25 km^2. These data were retrieved with the empirical CMOD5 GMF (Hersbach et al., 2007). Comparisons with independent mooring and shipboard observations demonstrate the good accuracy of ASCAT wind data (Bentamy et al., 2008).

Both ASCAT and HYSCAT are in quasi sun-synchronous orbits. The HYSCAT local equator crossing time at the descending node is 6:00 A.M., whereas that of ASCAT is 9:30 A.M. The spatially and temporally collocated data are available at high latitudes owing to these different local equator crossing times. In this study, the temporal and spatial differences between HYSCAT and ASCAT collocated data were set to be within 1 h and 25 km, respectively.

2.3 Buoy data

For comparison with the HYSCAT wind data, we collected buoy observations from buoys operated by the National Data Buoy Center (NDBC) and the Tropical Atmosphere Ocean (TAO) project. The locations of the buoys are shown in Fig.1. Only the buoys moored offshore and in deep water were selected; in the present study, offshore was defined as at least 50 km off the coast, while water depths over 50 m were considered to be deep water.

Most remote sensors measure wind speed at 10 m standard height. Buoy measurements of wind velocity, sea surface and air temperature, and humidity have been utilized to calculate wind speed at 10 m height according to the COARE3.0 algorithm (Fairall et al., 2003). The temporal interval of the NDBC and standard TAO buoy observations is 10 min. Details of the buoys, instruments, and stations were introduced by Meindl and Hamilton (1992) and McPhaden et al. (1998). The HYSCAT data and buoy observations were collocated with temporal and spatial differences of no more than 30 min and 25 km, respectively.

2.4 Gridded model data

The NCEP fields we used were the Global Data Assimilation System (GDAS) 1°×1° 1 000 mbar surface winds. The NCEP winds were interpolated to the location and time of the HYSCAT wind vectors by trilinear interpolation. Trilinear interpolation is a method of conducting multivariate interpolation on a three-dimensional regular grid and is frequently used in numerical data analysis. The trilinear interpolation method has been used previously in scatterometer-model comparison (Chelton and Freilich, 2005).

3 RESULT AND DISCUSSION

3.1 Comparison with buoy observations

The scatterometer wind speed and direction observed by HYSCAT were compared with data from in situ buoys. In particular, a statistical comparison was performed using density plots. Figure 2 depicts the density plots for wind speed and direction against collocated buoy observations over the tropics and the Northern Hemisphere using TAO and NDBC buoys, respectively. In general, the wind speed and direction derived from HYSCAT were in agreement with the buoy observations.

The standard parameters (mean bias error: Bias;

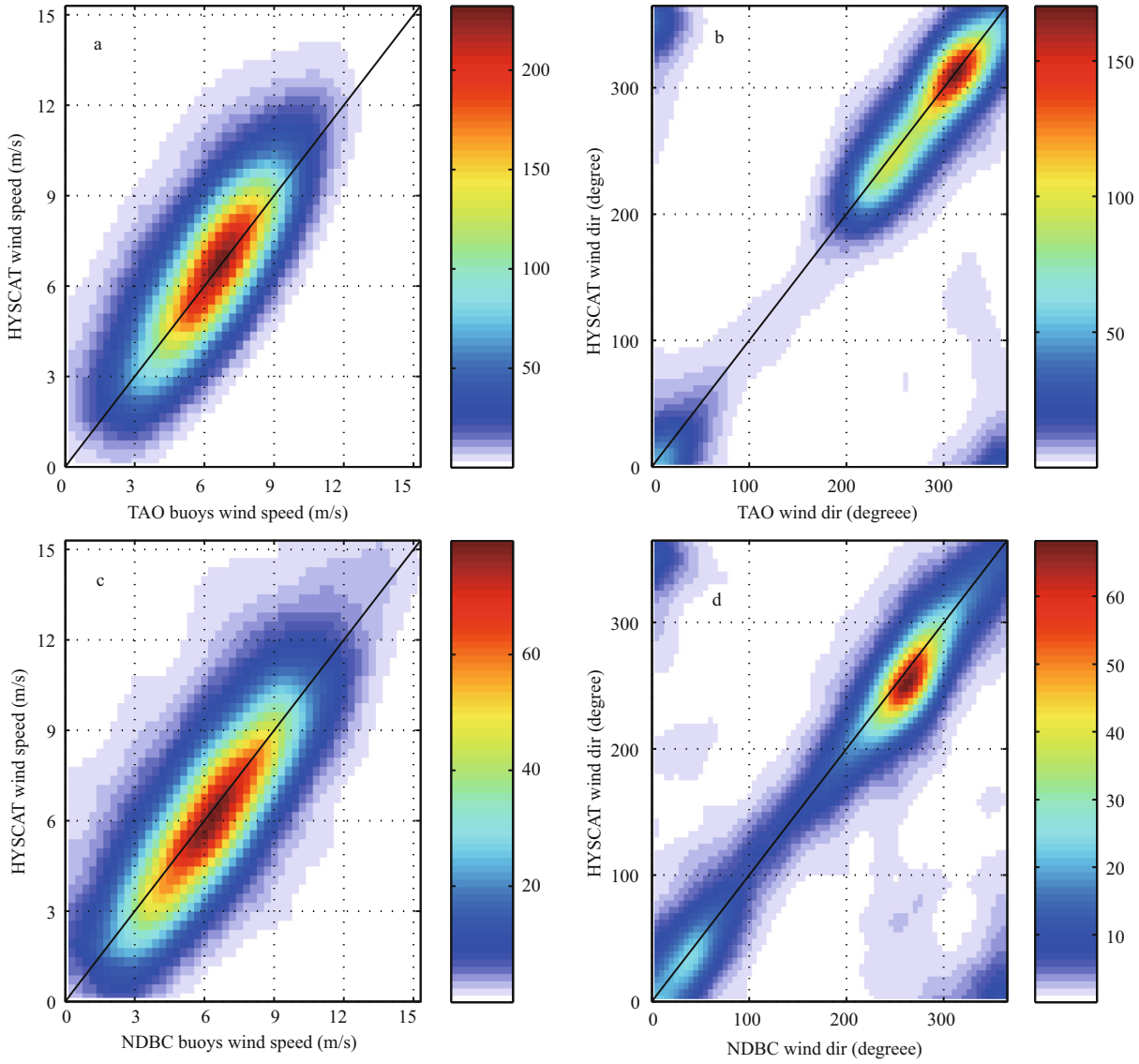

Fig.2 Comparison of winds retrieved from HYSCAT and winds observed from the TAO (a and b) and NDBC (c and d) buoys

The colors of the density plots represent the number of data points in the corresponding grid.

Table 1 Statistical parameters for the comparison of HYSCAT and buoys (TAO and NDBC buoys) for different wind speed ranges

Wind speed (m/s)		Bias (mean residual)		RMSE		Correlation coefficient	
		Speed	Direction	Speed	Direction	Speed	Direction
TAO	All	0.59	7.68	2.11	25.75	0.86	0.82
	<5	-0.42	15.68	2.85	40.56	0.75	0.70
	5–10	0.57	8.85	1.95	22.51	0.89	0.84
	>10	0.62	4.54	2.95	22.51	0.75	0.89
NDBC	All	0.27	5.60	1.83	20.05	0.90	0.85
	<5	-0.36	12.51	2.29	32.58	0.83	0.81
	5–10	0.25	6.36	1.72	20.81	0.93	0.85
	>10	0.43	4.04	1.96	18.85	0.87	0.92

root-mean-square error: RMSE; correlation coefficient: R) for the comparisons over different wind speed ranges were calculated and are summarized in Table 1. These parameters were calculated separately over the tropics (20°S–20°N) using TAO data and over the Northern Hemisphere (20°–70°N) using NDBC data. The RMSEs over the full wind range are 2.11 m/s for TAO buoys and 1.83 m/s for NDBC buoys. For wind direction, the RMSEs are 25.75° and 20.05° for TAO and NDBC buoys, respectively. As for wind speed, the RMSE of wind direction for TAO buoys is larger than that for NDBC buoys. All other statistical parameters, i.e., the bias and correlation coefficient, exhibit similar results for TAO and NDBC data.

One possible reason for the larger RMSE for the HYSCAT-TAO collocation than for the HYSCAT-NDBC collocation is the lack of consideration of the effects of ocean currents. The scatterometers measure winds relative to the moving ocean surface, whereas the buoy anemometers measure winds over a fixed location. Dickinson et al. (2001) and Kelly et al. (2001) examined the effects of the surface current on scatterometer-retrieved wind vectors in the tropical Pacific using the TAO buoy data, demonstrating that scatterometer-retrieved wind speeds are underestimated when the wind and surface ocean current flow in the same direction and overestimated when they flow in opposite directions. Thus, the large tropical current system may have resulted in larger scatter for the TAO buoys than for the NDBC buoys. The impact of rain on the scatterometer wind fields may also account for the differences between the TAO and NDBC data. It is generally recognized that the presence of rain will degrade the quality of wind retrieval for scatterometers. Thus, the frequent precipitation in the Intertropical Convergence Zone (ITCZ) could have produced the large RMSE for the TAO buoys. However, additional data are required to clarify the mechanisms behind the observed differences.

Here, we focus on the performance of wind speed and direction retrieval at low speeds. For low wind speeds (<5 m/s), the RMSEs for wind direction are 40.56° for TAO and 32.58° for NDBC buoys, which implies that the HYSCAT-derived wind direction for low wind speeds is less accurate than that for the moderate to high wind speed ranges. A negative bias was observed for wind speed, indicating an underestimation of HYSCAT-derived wind speeds during low wind speed regimes. In fact, low wind speeds (<5 m/s) are not sufficiently strong to overcome viscous damping, such that Bragg waves cannot grow (Donelan and Pierson, 1987). It is one of reasons contribute to the large RMSEs obtained for both wind speed and direction for calm and light winds. For wind speeds >5 m/s, the RMSE for wind direction decreased quickly with increasing wind speed and a good correlation coefficient was achieved for the TAO data. Wind direction bias is also more apparent for HYSCAT winds at low wind speeds than for moderate and high wind speeds. For the NDBC data, the error statistics exhibited a similar trend.

3.2 Analysis of residuals

Both wind speed and wind direction residuals were also computed for HYSCAT data. These residuals represent the differences between the HYSCAT and buoy wind data. Figure 3 illustrates the dependencies of the wind speed and direction residuals (i.e., HYSCAT-buoy) on the buoy wind speed using a density plot. The wind speed residuals exhibit no obvious dependence on buoy wind speed over a wind speed range of 5–15 m/s.

For wind direction, the bias is large and varies between positive and negative values for low wind speeds (<4 m/s) and decreases as wind speed increases. Some attempts were made in previous studies (Dickinson et al., 2001; Ebuchi et al., 2002) to examine wind direction bias associated with Coriolis turning in the Ekman layer of the atmosphere and with other geophysical variables such as atmospheric stratification. However, these studies found no dependence of scatterometer wind direction bias on these variables.

Several previous studies have reported the dependence of scatterometer-measured backscattering on sea state (Keller et al., 1985; Ebuchi et al., 2002), sea surface temperature (Donelan and Pierson, 1987), and stability of the atmospheric boundary layer (Keller et al., 1985). To assess the influence of atmospheric and oceanic conditions on the quality of scatterometer-retrieved wind, the relationships between HYSCAT wind speed residuals and sea surface temperature (SST), SST minus air temperature, and significant wave height were investigated. The results show that the wind speed residuals exhibit weak dependencies on the significant wave height, while the SST and air-sea temperature differences are less correlated. These results imply that higher wind waves may cause enhanced radar backscattering under the same wind conditions.

3.3 Comparison with ASCAT

Wind vectors from HYSCAT and ASCAT were compared for the time period from January 1, 2012, to December 31, 2013. The temporal and spatial differences between HYSCAT and ASCAT were limited to within 1 h and 25 km, respectively, for quantitative comparison. The collocated data were found to be located at high latitudes owing to the different equator crossing times for HYSCAT and ASCAT. Figure 4 shows the density plot of the comparison between HYSCAT and ASCAT. The range of medium winds (5–15 m/s) constitutes the majority of the wind data population. Very few (approximately 1%) collocated data were found to be associated with high wind speeds (>15 m/s).

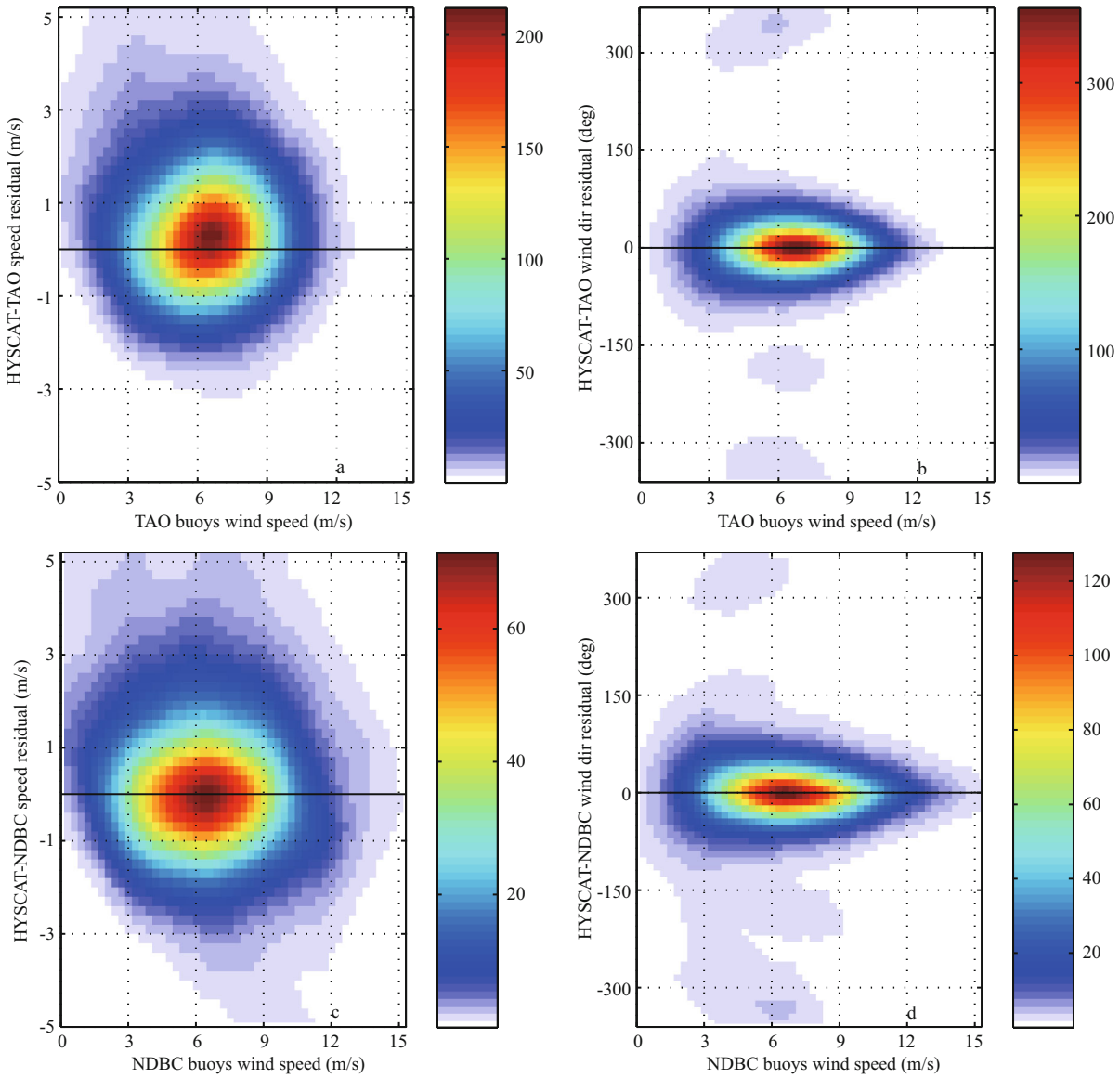

Fig.3 Comparison of wind speed and direction residuals (HYSCAT minus buoy data) for TAO buoys (a and b) and NDBC buoys (c and d)

Table 2 Statistical comparison of wind speed and direction between HYSCAT and ASCAT

	Wind speed			Wind direction		
Wind speed range	Bias	RMSE	Correlation coefficient	Bias	RMSE	Correlation coefficient
All	0.39	1.68	0.92	5.24	19.1	0.89
<5	0.50	2.20	0.81	10.41	27.26	0.75
5-10	0.31	1.43	0.94	5.83	17.26	0.89
>10	0.32	1.86	0.92	3.44	19.39	0.92

The overall HYSCAT-ASCAT comparison shows that wind data from both scatterometers are in good agreement, with RMSEs of 1.68 m/s for wind speed and 19.1° for wind direction for all of the collocated data. However, a slight overestimation of wind speed by ASCAT is apparent (Fig.4) for the entire wind speed range.

We also compared the collocated data for which the difference in acquisition time between HYSCAT and ASCAT was less than half an hour (not shown here). The computed RMSEs for wind speed and direction for these data are 1.67 m/s and 18.98°, respectively; these values are slightly lower than the RMSEs for the 1-h collocated data.

The statistical parameters of this comparison for different speed ranges are presented in Table 2. These results indicate that the lowest RMSEs (1.43 m/s for wind speed, 17.26° for wind direction) exist for the wind speed range 5–10 m/s.

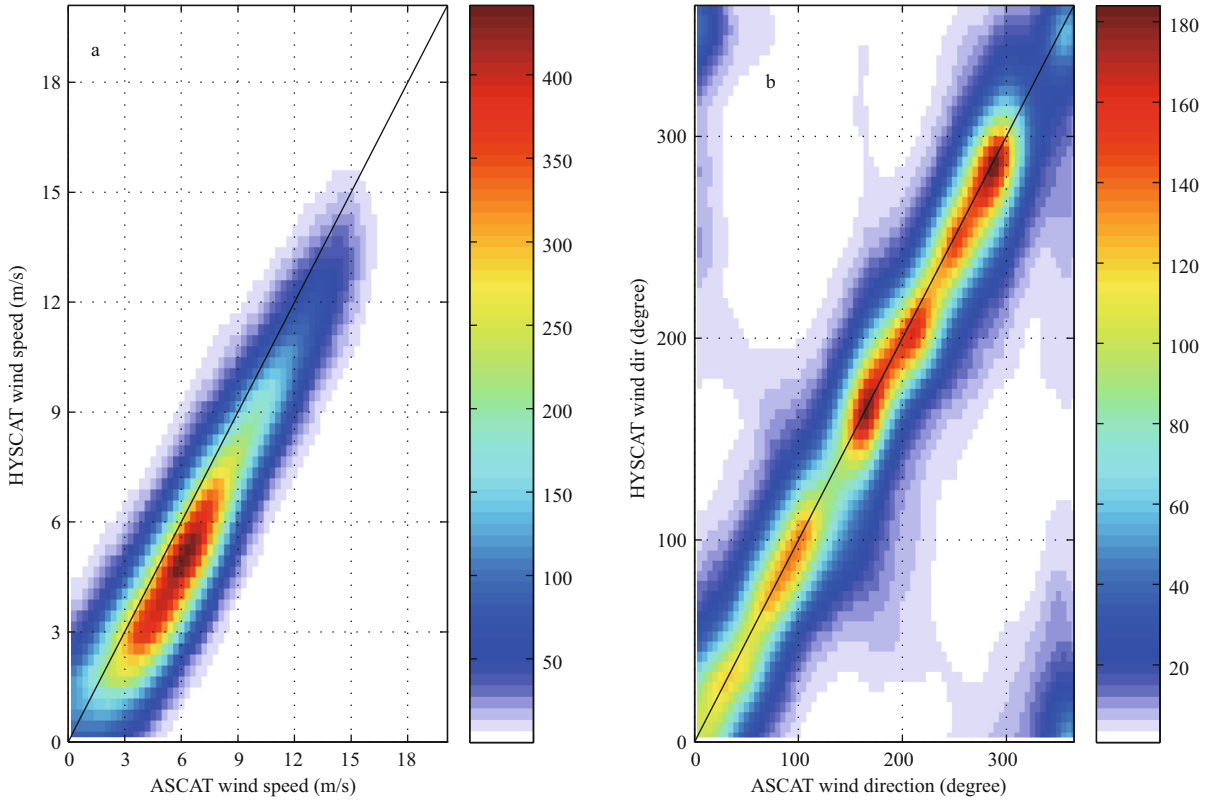

Fig.4 Comparison of wind speed (a) and direction (b) between HYSCAT and ASCAT

3.3 Comparison with NCEP model data

3.3.1 Spatial distribution

Above, we have demonstrated the good agreement of HYSCAT data with in-situ buoy observations and ASCAT measurements. The statistics computed by collocating scatterometer winds with buoy and ASCAT winds may not represent the error distribution globally, because the buoys offer limited spatial sampling distribution and the HYSCAT-ASCAT collocated data are limited to high latitudes. Thus, we also compared HYSCAT winds with the 6-h numerical forecast winds from the NCEP. HYSCAT winds were binned into the NCEP spatial resolution (1°) at each NCEP grid point. The average number of collocated pairs used for comparison exceeded 1 000 for each grid points. The global spatial patterns of the bias and SD for the year 2012 were computed and are depicted in Fig.5.

As shown in Fig.5a, the mean bias between collocated HYSCAT and NCEP wind speed (Bias=U_{HYSCAT}–U_{NCEP}) is generally less than 1 m/s for the global ocean. In general, bias values >0 were found in the tropical to mid-latitudes, with values in the range 0.50–0.80 m/s. The spatial pattern of bias >0 resembles that of tropical and mid-latitude storm track precipitation. In contrast to the tropics or mid-latitudes, bias is negative at subpolar and polar latitudes. This is particularly pronounced at southern latitudes, where the difference may exceed 0.4 m/s. SD was found to be larger in the mid-latitudes and tropics than in the subpolar and polar regions (Fig.5b). Moreover, SD is generally greater than 1.5 m/s in the zones of the mid-latitude storm tracks in both hemispheres, but is smaller than 1 m/s in the subpolar regions. In the mid-latitude regions of the South Indian Ocean and North Pacific Ocean, SD exhibits a maximum value of up to 2 m/s. As discussed by Ebuchi et al. (2002), convection events in the tropics and strong wind in the mid-latitude storm tracks may contribute to the spatial SD distribution for scatterometers.

3.3.2 Density plots

Figure 6 shows density plots for scatterometer winds from HYSCAT with respect to NCEP wind for one swath. It was found that the most of the collocated data correspond to the low and moderate wind speed ranges.

The statistical parameters of HYSCAT winds with

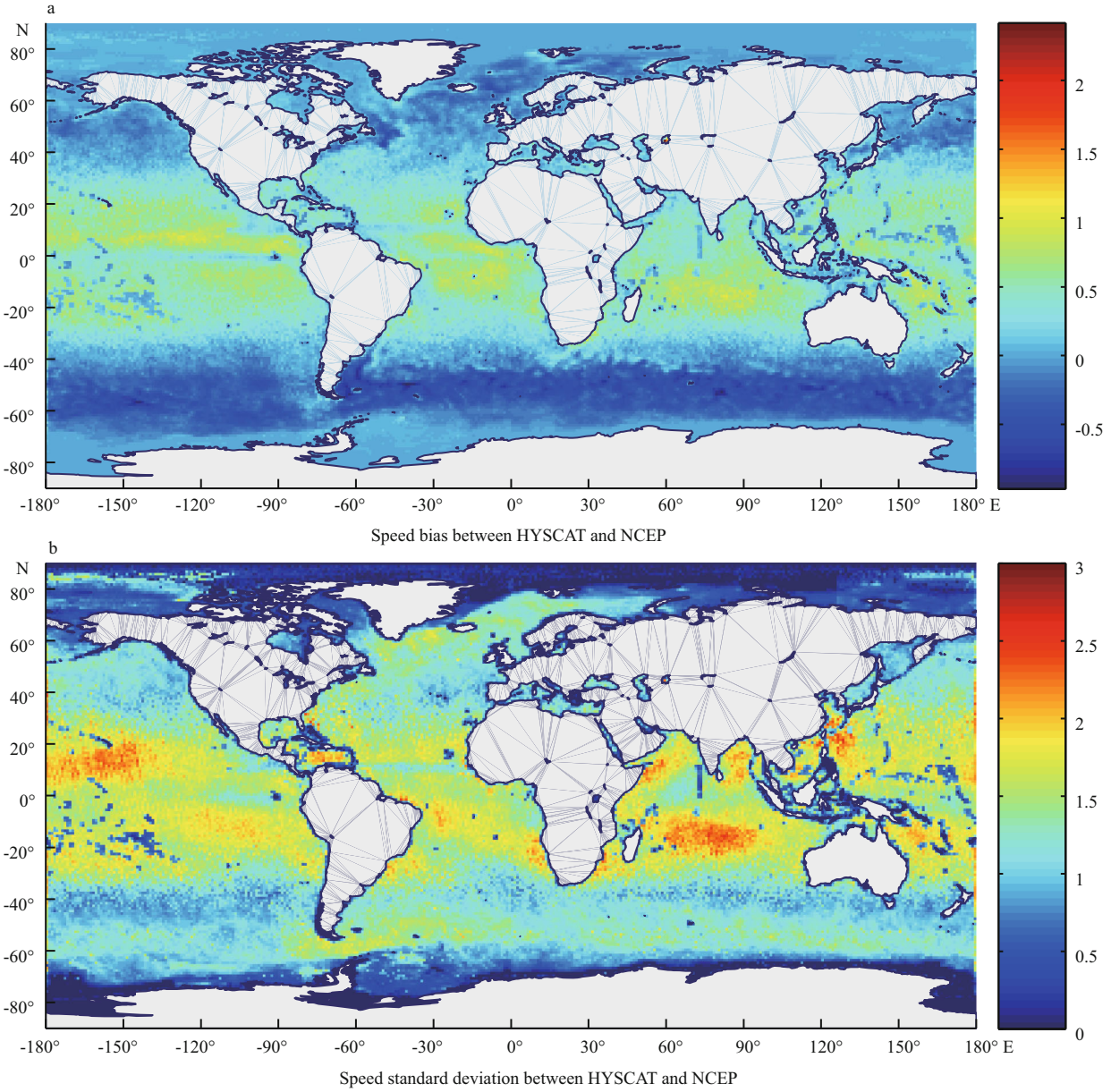

Fig.5 Wind speed mean bias (a) and standard deviation (SD) (b) between collocated HYSCAT and NCEP for the year 2012

Table 3 Statistical comparison of wind speed and direction between HYSCAT and NCEP model data

	Bias		RMSE		Correlation coefficient	
Regions	Speed	Direction	Speed	Direction	Speed	Direction
Northern Hemisphere	0.93	5.8	2.2	19	0.86	0.84
Tropics	1.5	11	2.8	27	0.79	0.73
Southern Hemisphere	0.5	7.1	2.1	22	0.83	0.81

respect to the NCEP over the Northern Hemisphere (20°–90°N), the tropics (20°S–20°N), and the Southern Hemisphere (20°–90°S) are presented in Table 3. It is clear that HYSCAT winds perform better in the Northern Hemisphere and Southern Hemisphere than over the tropics. In particular, the RMSEs of wind speed and direction over the tropics are greater than those for both the Northern Hemisphere and Southern Hemisphere. For the northern band, the RMSEs of the wind speed and direction are approximately 2.2 m/s and 19°, respectively, with bias of approximately 0.93 m/s and approximately 5.8° for speed and direction, respectively. For the tropics, the RMSEs of wind speed and direction are approximately 2.8 m/s and 27°, respectively, with respective biases of approximately 2.8 m/s and 27°. For the southern band, the RMSEs of wind speed and

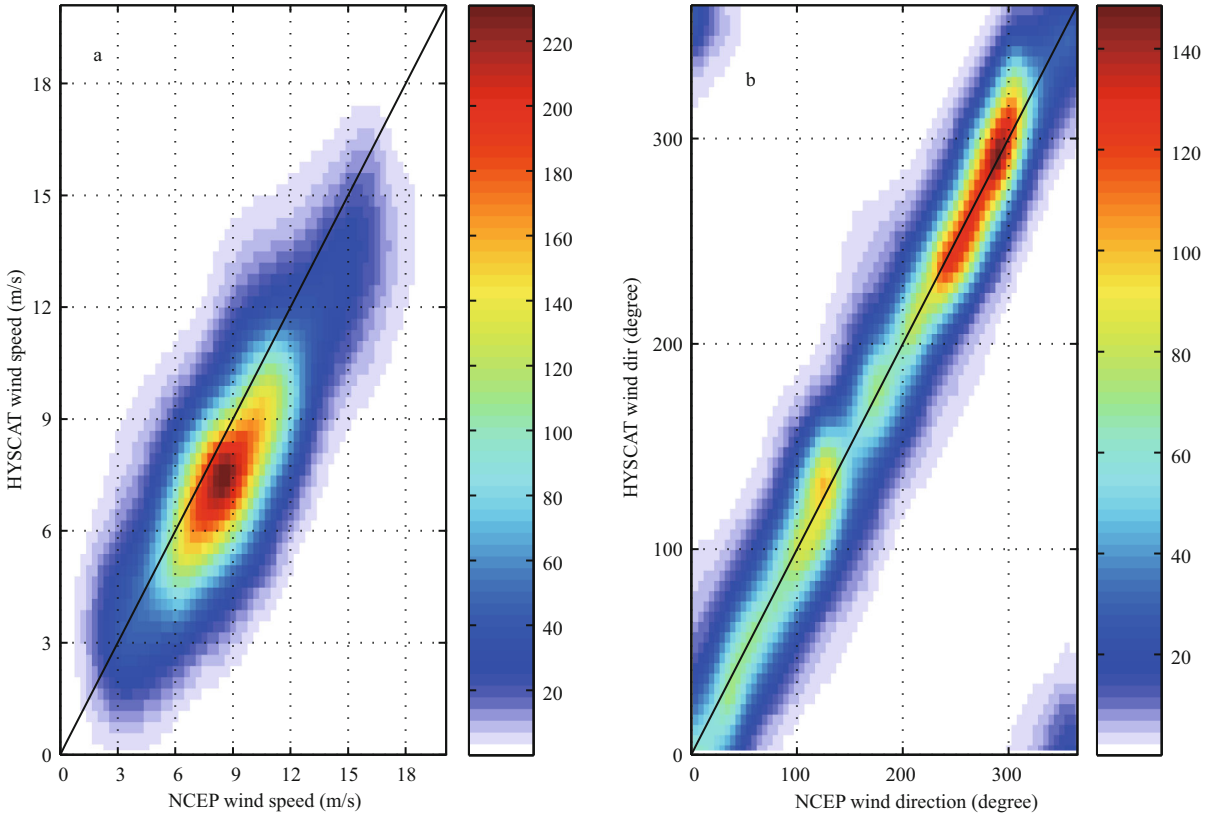

Fig.6 Density plot for HYSCAT winds speeds (a) and directions (b) with respect to NCEP model winds for March 1, 2012

Color scales indicate the numbers of collocated data.

direction are approximately 2.1 m/s and 22°, respectively, with respective biases of approximately 0.5 m/s and 7.1°.

4 CONCLUSION

Wind vectors observed by HYSCAT were compared with ocean buoy in situ observations, ASCAT measurements, and NCEP numerical model data to evaluate the quality of HYSCAT products. For the wind speed comparison, the RMSE is 2.11 m/s for the TAO data and 1.83 m/s for the NDBC data. No wind-speed-dependent systematic biases are discernible. For the wind direction comparison, the RMSE is approximately 25.75° for TAO and 20.05° for NDBC. Moreover, the RMSE of wind direction decreases with increasing wind speed.

The comparison between HYSCAT and ASCAT yielded RMSEs of 1.68 m/s for wind speeds and 19.1° for wind direction. To assess the quality of wind retrieval on a global scale, the HYSCAT data were also compared with reanalysis data from the NCEP. The results show that the RMSEs of the speed and direction of HYSCAT winds are 2.6 m/s and 26°, respectively. The global distribution of residuals (HYSCAT-NCEP) demonstrates the effects of rain and other meso-scale atmospheric phenomena on scatterometer wind retrieval. Considering the large temporal and spatial differences between the collocated HYSCAT and the in situ observations, it is concluded that the mission requirements for wind speed and direction have been satisfied. The HYSCAT-retrieved data will be useful for future scientific study and for weather prediction applications.

5 ACKNOWLEDGEMENT

We would like to thank the National Satellite Ocean Application Service (NSOAS), State Oceanic Administration (SOA), People's Republic of China, for the distribution of the HYSCAT data, EUMETSAT for the distribution of the ASCAT data, and the Global Data Assimilation System (GDAS) for the distribution of the NCEP data.

References

Bentamy A, Croize-Fillon D, Perigaud C. 2008. Characterization of ASCAT measurements based on buoy and QuikSCAT wind vector observations. *Ocean Science*, **4**(4): 265-274, http://dx.doi.org/10.5194/os-4-265-2008.

Bourassa M A, Freilich M H, Legler D M, Liu W T, O'Brien J J. 1997. Wind observations from new satellite and research vessels agree. *EOS*, *Transactions American Geophysical Union*, **78**(51): 597-602, http://dx.doi.org/10.1029/97EO00357.

Bourassa M A, Legler D M, O'Brien J J, Smith S R. 2003. SeaWinds validation with research vessels. *Journal of Geophysical Research*: *Oceans* (*1978-2012*), **108**(C2): 3 019, http://dx.doi.org/10.1029/2001JC001028.

Chelton D B, Freilich M H. 2005. Scatterometer-based assessment of 10-m wind analyses from the operational ECMWF and NCEP numerical weather prediction models. *Monthly Weather Review*, **133**(2): 409-429, http://dx.doi.org/10.1175/MWR-2861.1.

Dickinson S, Kelly K A, Caruso M J, McPhaden M J. 2001. Comparisons between the TAO buoy and NASA scatterometer wind vectors. *Journal of Atmospheric and Oceanic Technology*, **18**(5): 799-806, http://dx.doi.org/10.1175/1520-0426(2001)018<0799:CBTTBA>2.0.CO;2.

Donelan M A, Pierson W J Jr. 1987. Radar scattering and equilibrium ranges in wind-generated waves with application to scatterometry. *Journal of Geophysical Research*: *Oceans* (*1978-2012*), **92**(C5): 4 971-5 029, http://dx.doi.org/10.1029/JC092iC05p04971.

Dong X L, Lang S Y, Wang T, Liu H G. 2007. Accuracy and resolution analysis of the pencil beam radar scatterometer onboard China's HY-2 satellite. *In*: IGARSS 2007. IEEE International Geoscience and Remote Sensing Symposium. IEEE, Barcelona. p.4 467-4 470, http://dx.doi.org/10.1109/IGARSS.2007.4423847.

Draper D W, Long D G. 2002. An assessment of SeaWinds on QuikSCAT wind retrieval. *Journal of Geophysical Research*: *Oceans* (*1978-2012*), **107**(C12): 5-1-5-14, http://dx.doi.org/10.1029/2002JC001330.

Ebuchi N. 1999. Statistical distribution of wind speeds and directions globally observed by NSCAT. *Journal of Geophysical Research*: *Oceans* (*1978-2012*), **104**(C5): 11 393-11 403, http://dx.doi.org/10.1029/98JC02061.

Ebuchi N, Graber H C, Caruso M J. 2002. Evaluation of wind vectors observed by QuikSCAT/SeaWinds using ocean buoy data. *Journal of Atmospheric & Oceanic Technology*, **19**(12): 2 049-2 062, http://dx.doi.org/10.1175/1520-0426(2002)019<2049:EOWVOB>2.0.CO;2.

Fairall C W, Bradley E F, Hare J E, Grachev A A, Edson J B. 2003. Bulk parameterization of air-sea fluxes: updates and verification for the COARE algorithm. *Journal of Climate*, **16**(4): 571-591, http://dx.doi.org/10.1175/1520-0442(2003)016<0571:BPOASF>2.0.CO;2.

Freilich M H, Dunbar R S. 1999. The accuracy of the NSCAT 1 vector winds: comparisons with National Data Buoy Center buoys. *Journal of Geophysical Research*: *Oceans* (*1978-2012*), **104**(C5): 11 231-11 246, http://dx.doi.org/10.1029/1998JC900091.

Hersbach H, Stoffelen A, De Haan S. 2007. An improved C-band scatterometer ocean geophysical model function: CMOD5. *Journal of Geophysical Research*: *Oceans* (*1978-2012*), **112**(C3): C03006, http://dx.doi.org/10.1029/2006JC003743.

Jiang X W, Lin M S, Liu J Q, Zhang Y G, Xie X T, Peng H L, Zhou W. 2012. The HY-2 satellite and its preliminary assessment. *International Journal of Digital Earth*, **5**(3): 266-281, http://dx.doi.org/10.1080/17538947.2012.658685.

Keller W C, Plant W J, Weissman D E. 1985. The dependence of X band microwave sea return on atmospheric stability and sea state. *Journal of Geophysical Research*: *Oceans* (*1978-2012*), **90**(C1): 1 019-1 029, http://dx.doi.org/10.1029/JC090iC01p01019.

Kelly K A, Dickinson S, McPhaden M J, Johnson G C. 2001. Ocean currents evident in satellite wind data. *Geophysical Research Letters*, **28**(12): 2 469-2 472, http://dx.doi.org/10.1029/2000GL012610.

Li D W, Shen H. 2014. Construction of geophysical model function for a platform-borne C-band microwave scatterometer. *Ocean Engineering*, **84**: 157-163, http://dx.doi.org/10.1016/j.oceaneng.2014.04.012.

Liu W T. 2002. Progress in scatterometer application. *Journal of Oceanography*, **58**(1): 121-136, http://dx.doi.org/10.1023/A:1015832919110.

Long D G, Endel J M. 1991. Identifiability in wind estimation from scatterometer measurements. *IEEE Transactions on Geoscience and Remote Sensing*, **29**(2): 268-276, http://dx.doi.org/10.1109/36.73668.

Masuko H, Arai K, Ebuchi N, Konda M, Kubota M, Kutsuwada K, Manabe T, Mukaida A, Nakazawa T, Nomura A. 2000. Evaluation of vector winds observed by NSCAT in the seas around Japan. *Journal of Oceanography*, **56**(5): 495-505, http://dx.doi.org/10.1023/A:1011192725800.

McPhaden M J, Busalacchi A J, Cheney R, Donguy J R, Gage K S, Halpern D, Ji M, Julian P, Meyers G, Mitchum G T, Niiler P P, Picaut J, Reynolds R W, Smith N, Takeuchi K. 1998. The Tropical Ocean-Global Atmosphere observing system: a decade of progress. *Journal of Geophysical Research*: *Oceans* (*1978-2012*), **103**(C7): 14 169-14 240, http://dx.doi.org/10.1029/97JC02906.

Meindl E A, Hamilton G D. 1992. Programs of the national data buoy center. *Bulletin of the American Meteorological Society*, **73**(7): 985-993, http://dx.doi.org/10.1175/1520-0477(1992)073<0985:POTNDB>2.0.CO;2.

Offiler D. 1994. The calibration of Ers-1 satellite scatterometer winds. *Journal of Atmospheric and Oceanic Technology*, **11**(4): 1 002-1 017, http://dx.doi.org/10.1175/1520-0426(1994)011<1002:TCOSSW>2.0.CO;2.

Risien C M, Chelton D B. 2008. A global climatology of surface wind and wind stress fields from eight years of QuikSCAT scatterometer data. *Journal of Physical Oceanography*, **38**(11): 2 379-2 413, http://dx.doi.org/10.1175/2008JPO3881.1.

Wentz F J, Smith D K. 1999. A model function for the ocean-normalized radar cross section at 14 GHz derived from NSCAT observations. *Journal of Geophysical Research*: *Oceans* (*1978-2012*), **104**(C5): 11 499-11 514, http://dx.doi.org/10.1029/98JC02148.